DENSITY VARIATIONS OVER SUBPARSEC SCALES IN DIFFUSE MOLECULAR GAS

K. PAN,[1,2] S. R. FEDERMAN,[1,2] AND D. E. WELTY[3,4]

ABSTRACT

We present high-resolution observations of interstellar CN, CH, CH$^+$, Ca I, and Ca II absorption lines toward the multiple star systems HD 206267 and HD 217035. Substantial variations in CN absorption are observed among three sight lines of HD 206267, which are separated by distances of order 10,000 AU; smaller differences are seen for CH, CH$^+$, and Ca I. Gas densities for individual velocity components are inferred from a chemical model, independent of assumptions about cloud shape. While the component densities can differ by factors of 5.0 between adjacent sight lines, the densities are always less than 5000 cm^{-3}. Calculations show that the derived density contrasts are not sensitive to the temperature or reaction rates used in the chemical model. A large difference in the CH$^+$ profiles (a factor of 2 in column density) is seen in the lower density gas toward HD 217035.

Subject headings: ISM: clouds — ISM: molecules — ISM: structure — stars: individual (HD 206267, HD 217035)

1. INTRODUCTION

Evidence for pervasive subparsec-scale structure in the diffuse interstellar medium (ISM) has been accumulating over the past three decades through radio and optical/ultraviolet observations. Observations of H I 21 cm absorption toward high-velocity pulsars (Frail et al. 1994) and toward extended extragalactic radio sources (Faison & Goss 2001) reveal variations in optical depth on scales of 10–100 AU. Radio observations of absorption from H$_2$CO and OH toward extragalactic sources (Moore & Marscher 1995) also show changes in optical depth over time. Multiepoch optical measurements provide another probe of these small-scale structures (e.g., Lauroesch, Meyer, & Blades 2000; Price, Crawford, & Barlow 2000; Crawford et al. 2000; Welty & Fitzpatrick 2001). On intermediate scales of 10^2–10^5 AU, optical/ultraviolet observations of interstellar absorption lines (mainly from the trace species Na I and K I) toward individual members of binary or multiple star systems (e.g., Meyer & Blades 1996; Watson & Meyer 1996; Lauroesch et al. 1998; Lauroesch & Meyer 1999, hereafter LM99) suggest ubiquitous structure. Structure on these scales is also implied by variations of Na I and K I absorption profiles toward members of clusters (e.g., Langer, Prosser, & Sneden 1990; Bates et al. 1995) and toward bright extended cores of globular clusters (Meyer & Lauroesch 1999; Andrews, Meyer, & Lauroesch 2001). In this Letter, we present optical spectra at a resolution of ~1.7 km s^{-1} that reveal differences in molecular profiles across two multiple star systems.

While it is well established that the column densities of some atomic (H I, Na I, K I) and molecular (H$_2$CO, OH) species vary on scales of 10–10^5 AU in diffuse sight lines, detailed information on the physical conditions causing the variations is generally not available. A key question posed by the observations is whether the subparsec structure is caused by density variations (e.g., Frail et al. 1994; LM99; Crawford et al. 2000), by fluc-

tuations in ionization equilibrium (LM99; Welty & Fitzpatrick 2001), by the geometric structure of clouds (Heiles 1997), or by something else. A crucial point is to determine accurate physical conditions for the gas showing variations in column density. As a step in this direction, we present high-resolution absorption spectra of CN, CH, CH$^+$, Ca I, and Ca II, discuss the observed velocity component structure, and derive gas densities of components based on a simplified chemical model for CH, C$_2$, and CN (Federman et al. 1994; Knauth et al. 2001). We also investigate the sensitivity of the derived densities on cloud temperature and chemical reaction rates.

2. OBSERVATIONS AND DATA REDUCTION

High-resolution spectra were obtained for two multiple star systems in the active star-forming regions Cep OB2 and OB3 (Table 1). Most of the observations were acquired in 2000 September with the 2d-coudé spectrograph on the 2.7 m telescope at McDonald Observatory (Tull et al. 1995). A cross-disperser and the availability of a thin Textronix 2048 × 2048 CCD made it possible to get CN, CH, CH$^+$, Ca I, and Ca II features in a single exposure. In order to achieve a final signal-to-noise ratio (S/N) greater than 50, five 30 minute exposures were obtained for each target. Comparison spectra from a Th-Ar hollow cathode lamp were taken every 2 hr, while biases and flat fields were acquired each night. Dark frames were also obtained as a check on the amount of thermal noise from the cooled CCD. The setup yielded a spectral resolution of ~1.7 km s^{-1} that was determined from the widths of the Th-Ar lines. The star HD 206267A was observed in 1995 with the 0.9 m coudé feed telescope at Kitt Peak National Observatory. Spectra for K I, Ca II, CN, and CH were obtained using camera 6, the echelle grating, and the F3KB CCD, at resolutions of about 1.3 km s^{-1}. Comparison of K I spectra of HD 206267A obtained in 1995, 1998, and 2001 reveal no obvious temporal variation.

The raw images were reduced in the usual manner with the NOAO IRAF echelle data reduction package. The individual frames were first bias-subtracted. Cosmic-ray hits and scattered light were removed from each stellar image and flat field. The flat fields were divided into the stellar images to account for differences in pixel-to-pixel sensitivity. Since each echelle order was a few pixels wide, the orders were summed across this

[1] Department of Physics and Astronomy, University of Toledo, Toledo, OH 43606.

[2] Guest Observer, McDonald Observatory, University of Texas at Austin.

[3] Department of Astronomy and Astrophysics, University of Chicago, 5640 South Ellis Avenue, Chicago, IL 60637.

[4] Visiting Observer, Kitt Peak National Observatory, National Optical Astronomy Observatories, which is operated by AURA, Inc., under cooperative agreement with the National Science Foundation.

SYSTEM	V (mag)	E(B−V) (mag)	D (pc)	SEPARATION		REFERENCES
				arcsec	AU	
HD 206267A/C/D	5.7/8.0/7.9	0.52/0.57/0.42	615 ± 15	11.8 (A/C)	7250	1, 2
				31.6 (C/D)	19410	
				19.9 (A/D)	12220	
HD 217035A/B	8.6/8.6	0.76/0.76	725	1.9	1380	3, 4

REFERENCES.—(1) Perryman 1997; (2) de Zeeuw et al. 1999; (3) Crawford & Barnes 1970; (4) Dommanget & Nys 1994.

width. Then all extracted one-dimensional spectra were calibrated in wavelength using the Th-Ar comparison spectra. After correcting for Doppler motion, individual spectra for each sight line were combined. Finally, the combined spectra were normalized to unity using low-order polynomials. Final spectra appear in Figures 1 and 2; their S/Ns range from 50 to 150.

Component structure is clearly seen in the spectra. The equivalent width, W_λ, for each velocity component was determined by a Gaussian fit. We attempted to use the same velocity structure to fit all the absorption features in all lines of sight in each stellar system. While very good fits for HD 217035A/B and HD 206267A/C were obtained with essentially the same component structures, a slightly different component structure was required to fit the spectra of HD 206267D. For each sight line, however, the same velocity components are used for all species. Toward HD 206267C, for example, CN, CH, CH$^+$, Ca I, and Ca II all have components at about −3.1 and 0.9 km s^{-1}. The adopted velocity components for each species are indicated in Figures 1 and 2.

Each value of W_λ for the CH and CN components was converted into a column density using curves of growth. The Doppler parameter (b-value) was set at 1.0 km s^{-1} (Federman et al. 1994), a value consistent with the measured line widths. The inferred optical depths at line center were found to be modest (≤ 1). Therefore, our column densities are not susceptible to unresolved structure. Moreover, even for a b-value of 0.5 km s^{-1}, the column density ratio between sight lines for a given velocity component—from which the density contrasts are inferred—changes by only 15%. When only the $R(0)$ line of CN at 3874.61 Å was detected for a component, the column density N(CN) for the component was set equal to 1.5 times the value from $R(0)$, as would be expected for an excitation temperature of about 2.7 K. If a CH component was detected but with no corresponding CN absorption, a 3 σ detection limit is given. Table 2 lists the column densities for the HD 206267 system,
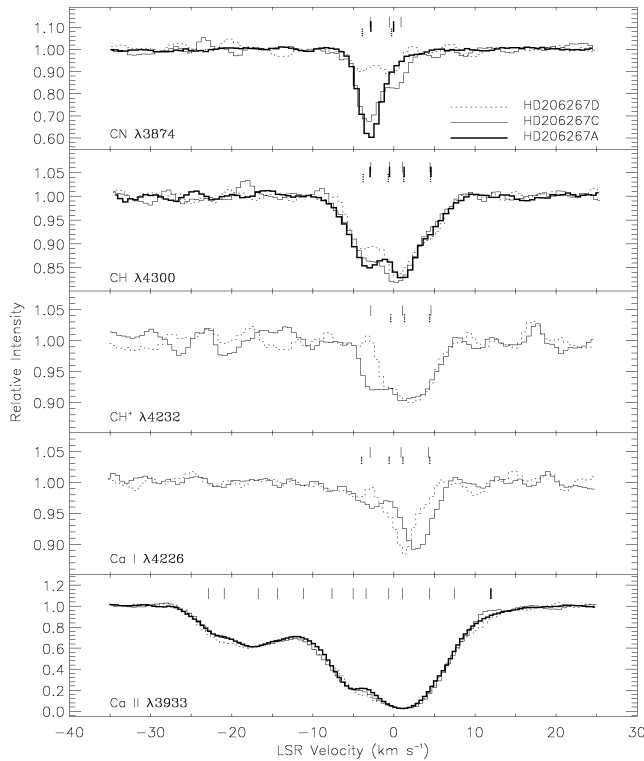

FIG. 1.—Absorption from interstellar CN, CH, CH$^+$, Ca I, and Ca II in the spectra of HD 206267A (*thick solid lines*), HD 206267C (*solid lines*), and HD 206267D (*dotted lines*). The observed line is indicated. Note that the relative intensity scales for the panels differ. Hash marks above each spectrum show the component structure derived from Gaussian fits.
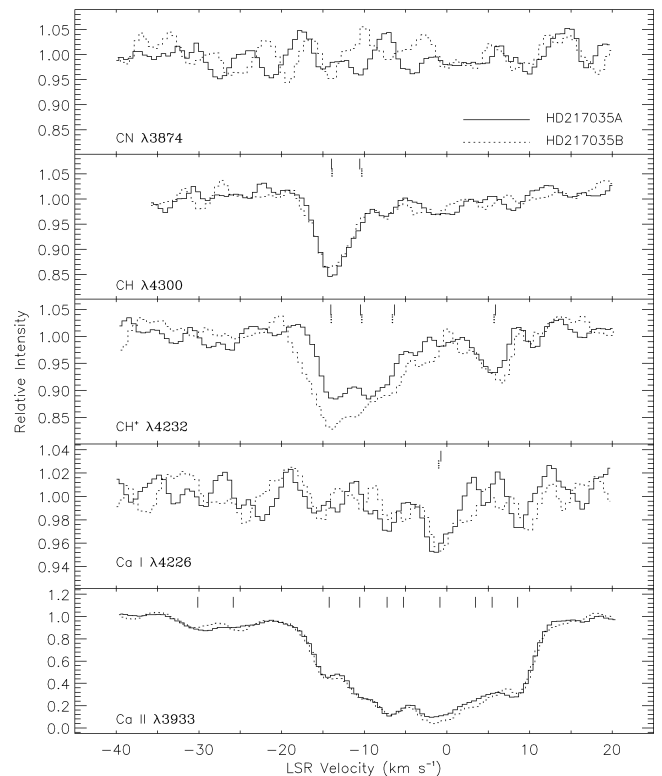

FIG. 2.—Same as Fig. 1, but for HD 217035A (*solid lines*) and HD 217035B (*dotted lines*).

TABLE 2
Column Densities and Densities for the HD 206267 System

Sight Line	Quantity	v_{LSR} (km s^{-1})				
		−4.1	−3.1	−0.7	0.9	4.3
HD 206267A	N(CN)	...	7.0 ± 0.2	0.9 ± 0.2	<0.2	<0.2
	N(CH)	...	14.8 ± 0.5	3.6 ± 0.3	10.8 ± 0.5	3.5 ± 0.3
	n	...	1500 ± 110	700 ± 120	<60	<170
HD 206267C	N(CN)	...	4.9 ± 0.3	0.9 ± 0.2	1.8 ± 0.3	<0.3
	N(CH)	...	12.5 ± 0.8	2.4 ± 0.5	10.7 ± 0.8	3.8 ± 0.6
	n	...	1000 ± 200	1100 ± 500	400 ± 90	<180
HD 206267D	N(CN)	1.3 ± 0.2	...	1.4 ± 0.2	<0.3	<0.3
	N(CH)	6.7 ± 0.4	...	4.5 ± 0.4	8.0 ± 0.4	7.1 ± 0.5
	n	600 ± 130	...	950 ± 220	<130	<150

Note.—N(CN) and N(CH) are in units of 10^{12} cm^{-2}, and n is in units of cm^{-3}.

where we find significant variations in these quantities; a complete listing of results will appear elsewhere.

3. ANALYSIS AND RESULTS

3.1. *Spectral Appearance*

Two members of multiple star system HD 206267 (C/D) were observed with the same instrumental setup. As shown in Figure 1, there are striking differences in the CN, CH, CH$^+$, and Ca I absorption profiles between the two sight lines. In addition to differences in component strengths, the Ca I profiles appear slightly "shifted" with respect to one another. Because CH$^+$ and Ca I absorption lines occur in the same echelle order, because the wavelength solutions for the two stars are the same, and because the CH$^+$ profiles toward the two stars match so well in velocity space, we conclude that the "shift" cannot be attributed to wavelength calibration. Since a slightly different component structure was required to get good fits for the CN and CH$^+$ profiles for the two sight lines, the shift is more likely the result of a slightly different component structure.

For comparison, the slightly higher resolution KPNO spectra of CN, CH, and Ca II toward HD 206267A were smoothed to the effective resolution of the spectra for HD 206267C/D. While Gaussian fits show that the interstellar absorption toward A and C exhibits the same component structure, large variations in line strength are found for both CN and CH. Significant variations are also seen between the spectra toward C and D for all observed species except Ca II. It is noteworthy that CN, which is a good tracer of dense gas (e.g., Federman et al. 1994), shows the largest variations.

Figure 2 shows significant differences in the CH$^+$ absorption profiles for the two members of the HD 217035 system, but the CH, Ca I, and Ca II profiles are very similar. Absorption from CN was not detected in either sight line. The CH$^+$ column densities (based on a curve of growth with b of 2.5 km s^{-1}) toward B are greater than the corresponding ones toward A by factors of 2.5, 1.5, 1.3, and 1.1 for the components at −14.3, 5.5, −10.5, and −6.7 km s^{-1}, respectively. In contrast, the CH and Ca I column densities for all components show no variations between the two sight lines at the 10% level.

3.2. *Chemical Modeling*

The significance of the line profile variations in Figures 1 and 2 and the column density variations seen in Table 2 is revealed through a simplified chemical model (Federman et al. 1994; Knauth et al. 2001), which provides estimates for the gas density in each component. The chemistry of the simple molecular species, CH, C$_2$, and CN, is relatively well understood (van Dishoeck & Black 1986; Federman et al. 1994); we use the formalism of Federman et al. (1994) in our analysis.

The fractional abundance of C$^+$ in diffuse gas, x(C$^+$) ∼ 1.4 × 10^{-4} (Sofia et al. 1997), is smaller by a factor of 1.8 than the value adopted by us in earlier studies (Federman & Huntress 1989; Federman et al. 1994). In order to preserve the rates needed to reproduce observations of C$_2$ and CN, the rate coefficients, k_1 (for C$^+$ + CH → C$_2^+$ + H) and k_5 (for C$^+$ + NH → all products), were correspondingly increased to 5.4 × 10^{-10} and 5.0 × 10^{-10} cm^3 s^{-1}, respectively. In addition, the grain optical depth corresponding to the transition from C$^+$ to CO was increased from 2.0 to 2.3; otherwise, gas densities somewhat larger than those typically found in diffuse molecular gas are obtained. All other input parameters remain unchanged. The derived gas densities for all components are listed in Table 2. Uncertainties are based on the ± 1 σ ranges in observed CH and CN columns. For the components at −3.1, −0.7, and 0.9 km s^{-1}, the chemical analysis provides evidence for factors of 1.5 to more than 5 changes in density as the cause of the CN profile variations seen in Figure 1, but in no case do we infer densities as large as 5000 cm^{-3}. While the CN excitation temperature can be used as an independent measure of the (electron) density (Black & van Dishoeck 1991), our data are not of sufficient precision for such an analysis.

4. DISCUSSION

Pervasive subparsec structure in the diffuse ISM, revealed by variations in atomic and molecular column densities, is beyond doubt. While other studies attempted to extract information on changes in physical condition related to these column density variations, the analyses were often based on the ad hoc assumption of a spherical cloud to determine the gas density structure. Moreover, the estimated densities are very sensitive to the temperature, which is generally not well known (Heiles 1997; Crawford et al. 2000). For instance, Crawford et al. (2000) used the column density ratio, N(K I)/N(Na I), to estimate the physical conditions in relatively dense clouds. Toward HD 81188, an increase in that ratio by a factor of 1.9, on a scale of ∼15 AU, could be explained either by increasing gas density by a factor of 5 or by decreasing temperature by a factor of 10. More likely, it may be due to some combination of density increase and temperature decrease. In many optical studies, an important unknown factor is the fractional ionization, which is needed to estimate N(H) from trace neutral species such as Na I (Lauroesch et al. 1998; Welty & Fitzpatrick 2001).

In our chemical analysis, the density is determined essentially

by a column density ratio, $N(CN)/N(CH)$, which reduces influences of cloud shape on density structure. For example, the -3.1 km s^{-1} component toward HD 206267C and the -0.7 km s^{-1} one toward HD 206267D have similar $N(CN)/N(CH)$—and thus comparable gas densities—even though their CN and CH column densities differ by a factor of about 3. Our derived gas density also is not sensitive to temperature. For instance, calculated densities for velocity components toward A and C increase by only 3%–8% when the temperature of 40 K is halved. The change in gas density *ratios* for a given velocity component in the two sight lines is even smaller, 1%–2%, when the temperature is halved.

Calculations also show that the gas density ratio for a given velocity component is not overly sensitive to the reaction rates in the chemical model. The rate coefficients k_1 and k_5 produce the largest effects on the gas density; decreasing either increases the calculated density. When both rate coefficients are decreased by 80%, the derived gas densities toward HD 206267A and HD 206267C increase by 50%–80%, but the gas density ratios for individual velocity components in the two sight lines change by only 4%–8%. The greatest change in this density ratio (from 1.58 to 1.72) is found for the -0.7 km s^{-1} component. We conclude that this chemical analysis is a good approach for deriving physical properties of small-scale structure in diffuse gas clouds with detectable amounts of CN.

The HD 206267 multiple star system is located in a region of recent, active star formation. LM99 studied K I variations toward members of this system and estimated typical gas density ratios of 1.1–2.7 for velocity components toward A and C. [Here we adopt $N(K\ I) \propto n^{2.7}$ instead of $n^{1.7}$ to take into account the additional factor of density in $N(K\ II)$.] The density ratios derived from CH and CN range from 1.5 to greater than 5.0. The lower density ratios found by LM99 presumably can be attributed to K I absorption probing a more extended volume of the cloud than CN absorption. The larger volume likely smooths out the large density variations in CN-rich gas. This picture is consistent with our Ca II observations, which show

no significant profile variations, probably because Ca II absorption occurs over an even more extended region (Crinklaw, Federman, & Joseph 1994; Welty, Morton, & Hobbs 1996). The present investigation also supports the conjecture of LM99 that much of the variation toward this system may be in dense gas. Table 2 shows that the gas density variations among the sight lines of the system are detected only in components with v_{LSR} from -4.0 to 1.0 km s^{-1}, with no obvious large density variation for the 4.3 km s^{-1} component. The CO emission-line maps of Patel et al. (1998) indicate that the CO-rich material in these lines of sight only appears within a velocity range of $v_{LSR} \sim -5.0$ to ~ 2.0 km s^{-1}—the range in which we see significant variations. Furthermore, using the K I results of LM99 with the trends determined by Welty & Hobbs (2001) for $N_{tot}(H)$, we find $N_{tot}(H)$ of $\approx 1 \times 10^{21}$ cm^{-2} for these components and only about 4×10^{20} cm^{-2} for the 4.3 km s^{-1} one. Our gas densities then suggest cloud thicknesses of about 1 pc along the lines of sight, similar to the sizes of the CO cloudlets seen in emission (Patel et al. 1998).

Variations in CN and CH column densities were not detected toward the HD 217035 system. Since only upper limits for CN are available for these sight lines, the density must be relatively low. The variations in the CH$^+$ profiles toward both systems may help to elucidate the uncertain chemistry for this molecule.

In summary, our observations of CN and CH absorption show that the diffuse molecular clouds toward the multiple star system HD 206267 exhibit significant density structure. The gas density varies by factors greater than 5.0 over a scale of $\sim 10,000$ AU. The present approach to studying small-scale structure in diffuse clouds provides reliable density contrasts, but it is limited to relatively dense molecule-rich clouds.

REFERENCES

Andrews, S. M., Meyer, D. M., & Lauroesch, J. T. 2001, ApJ, 552, L73
Black, J. H., & van Dishoeck, E. F. 1991, ApJ, 369, L9
Bates, B., Shaw, C. R., Kemp, S. N., Keenan, F. P., & Davies, R. D. 1995, ApJ, 444, 672
Crawford, D. L., & Barnes, J. V. 1970, AJ, 75, 952
Crawford, I. A., Howarth, I. D., Ryder, S. D., & Stathakis, R. A. 2000, MNRAS, 319, L1
Crinklaw, G., Federman, S. R., & Joseph, C. L. 1994, ApJ, 424, 748
de Zeeuw, P. T., Hoogerwerf, R., de Bruijne, J. H. J., Brown, A. G. A., & Blaauw, A. 1999, AJ, 117, 354
Dommanget, J., & Nys, O. 1994, Bull. Inf. CDS, 45, 7
Faison, M. D., & Goss, W. M. 2001, AJ, 121, 2706
Federman, S. R., & Huntress, W. T. 1989, ApJ, 338, 140
Federman, S. R., Strom, C. J., Lambert, D. L., Cardelli, J. A., Smith, V. V., & Joseph, C. L. 1994, ApJ, 424, 772
Frail, D. A., Weisberg, J. M., Cordes, J. M., & Mathers, C. 1994, ApJ, 436, 144
Heiles, C. 1997, ApJ, 481, 193
Knauth, D. C., Federman, S. R., Pan, K., Yan, M., & Lambert, D. L. 2001, ApJS, 135, 201
Langer, G. E., Prosser, C. F., & Sneden, C. 1990, AJ, 100, 216

Lauroesch, J. T., & Meyer, D. M. 1999, ApJ, 519, L181 (LM99)
Lauroesch, J. T., Meyer, D. M., & Blades, J. C. 2000, ApJ, 543, L43
Lauroesch, J. T., Meyer, D. M., Watson, J. K., & Blades, J. C. 1998, ApJ, 507, L89
Meyer, D. M., & Blades, J. C. 1996, ApJ, 464, L179
Meyer, D. M., & Lauroesch, J. T. 1999, ApJ, 520, L103
Moore, E. M., & Marscher, A. P. 1995, ApJ, 452, 671
Patel, N. A., Goldsmith, P. F., Heyer, M. H., Snell, R. L., & Pratap, R. 1998, ApJ, 507, 241
Perryman, M. A. C., ed. 1997, The *Hipparcos* and Tycho Catalogues (ESA SP-1200; Noordwijk: ESA)
Price, R. J., Crawford, I. A., & Barlow, M. J. 2000, MNRAS, 312, L43
Sofia, U. J., Cardelli, J. A., Guerin, K. P., & Meyer, D. M. 1997, ApJ, 482, L105
Tull, R. G., MacQueen, P. J., Sneden, C., & Lambert, D. L. 1995, PASP, 107, 251
van Dishoeck, E. F., & Black, J. H. 1986, ApJS, 62, 109
Watson, J. K., & Meyer, D. M. 1996, ApJ, 473, L127
Welty, D. E., & Fitzpatrick, E. L. 2001, ApJ, 551, L175
Welty, D. E., & Hobbs, L. M. 2001, ApJS, 133, 345
Welty, D. E., Morton, D. C., & Hobbs, L. M. 1996, ApJS, 106, 533